J Mater Sci (2007) 42:6287–6296
DOI 10.1007/s10853-006-1022-7

Preparation of lanthanum-doped TiO_2 photocatalysts by coprecipitation

Xuejun Quan · Huaiqin Tan · Qinghua Zhao · Xuemei Sang

Received: 9 March 2006 / Accepted: 25 September 2006 / Published online: 21 April 2007

Abstract The lanthanum-doped TiO_2 (La^{3+}-TiO_2) photocatalysts were prepared by coprecipitation and sol–gel methods. Rhodamine B was used as a model chemical in this work to evaluate the photocatalytic activity of the catalyst samples. The optimum catalyst samples were characterized by XRD, N_2 adsorption–desorption measurement, SEM and electron probe microanalyses to find their differences in physical and chemical properties. The experimental results showed that the La^{3+}-TiO_2 catalysts prepared by coprecipitation exhibited obviously higher photocatalytic activities as compared with that prepared by the conventional sol–gel process. The optimum photocatalysts prepared by the coprecipitation and sol–gel process have similar adsorption equilibrium constants in Rhodamine B solution and particle size distribution in water medium although there are larger differences in their surface area, morphology and pore size distribution. The pores in the sol-gel prepared catalysts are in the range of mesopores (2–50 nm), whereas the pores in the coprecipitation prepared catalysts consist of bigger mesopores and macropores (>50 nm). The morphology of the primary particles and agglomerates of the La^{3+}-TiO_2 catalyst powders was affected by doping processes. The inhibition effect of lanthanum doping on the phase transformation is greater in the coprecipitation process than in the sol–gel process, which could be related with the different amount of Ti–O–La bonds in the precursors. This finding could be used for preparing the anatase La^{3+}-TiO_2 catalysts with more regular crystal structure through a higher heat treatment temperature. The optimum amount of lanthanum doping is ca. 1.0 wt.% and the surface atomic ratio of [O]/[Ti] is ca. 2.49 for 1.0 wt.% La^{3+}-TiO_2 catalysts prepared by the two processes. The obviously higher photocatalytic activity of the La^{3+}-TiO_2 samples prepared by the coprecipitation could be mainly attributed to their more regular anatase structure and more proper surface chemical state of Ti^{3+} species. The optimum preparation conditions are 1.0 wt.% doping amount of lanthanum ions, calcination temperature 800 °C and calcination time 2 h using the coprecipitation process. As compared with the sol-gel process, the coprecipitation process used relatively cheap inorganic raw materials and a simple process without organic solvents. Therefore, the coprecipitation method provides a potential alternative in realizing large scale production.

Introduction

Over the last decade, the preparation and application of TiO_2 photocatalysts have been widely investigated in the fields of material science and environmental engineering because of its excellent photocatalytic activity, physical and chemical properties [1–12]. TiO_2 photocatalysts need the irradiation of ultraviolet light to produce photoinduced holes and electrons which play a crucial role in the degradation of organic pollutants; but there is only about 3–4% of ultraviolet light in sunlight.

In order to improve the photocatalytic activity of TiO_2 catalysts many modification methods have been developed, this includes doping other elements into TiO_2 photocatalysts. The photocatalytic activities were obviously enhanced in most cases [13–25]. The major doping methods include metal-photodepositing [13, 14], metal

X. Quan (✉) · H. Tan · Q. Zhao · X. Sang
Department of Chemical and Biological engineering, Chongqing Institute of Technology, Chongqing 400050, China
e-mail: hengjunq@cqit.edu.cn

ion-implantation [15], plasma CVD method [16, 17], sol–gel process [18], hydrothermal method [19–20] and wet impregnation method [21]. Using a simple wet process, Miyoshi et al. [22] prepared effective visible-light-active TiO_2 photocatalysts that contain a trace amount of nitrogen and have oxygen-deficient structure in grain boundaries.

As for doping elements, transition metals, such as Cr, Mn, V, Fe, Co, Ni and Cu etc., have been extensively used as dopants to enhance the photocatalytic performance of TiO_2 catalysts [13–15, 18–19, 21, 23–25], and the presence of the doping ions in the TiO_2 structure has caused a significant absorption shift to the visible region compared to pure TiO_2 powder (P25 Degussa) [24]. XPS analysis verified that the introduction of transition metals leads to changes of the electronic environment of Ti cations and the zeta-potential of oxides [25]. On the other hand, some researchers have reported that the doping of lanthanide ions into TiO_2 has unique functions for improving the photocatalyitc activity [26–32]. Xu and Li et al. [29, 31] have prepared lanthanum ion-doped TiO_2 photocatalysts by sol–gel processes and investigated the effects of doping lanthanide ions on the microstructure, surface chemical state and photocatalytic activity of the catalysts. Their investigation demonstrated that suitable content of doping lanthanide in TiO_2 can efficiently extend the light absorption properties to the visible region, enhance the photocatalytic activity to some extent compared with naked TiO_2, and cause an increase in adsorption capacity and interfacial electron transfer rate.

So far most of lanthanide ion-doped TiO_2 photocatalysts have been successfully prepared by using sol–gel processes. The sol–gel process usually needs relatively expensive titanium alkoxides as raw materials, such as tetra-n-butyl titanate etc.; and a lot of organic solvents such as methanol and ethanol. Most experimental results were also obtained on the basis of this process [27–29].

This work is aimed at investigating the preparation of lanthanum-doped TiO_2 (abbreviated as La^{3+}-TiO_2) photocatalysts by using a coprecipitation-calcination process, in which the chlorides of titanium and nitrate of lanthanum are used as raw materials.

Experimental

Preparation of photocatalysts

La^{3+}-TiO_2 catalysts prepared by coprecipitation

The La^{3+}-TiO_2 samples were prepared by coprecipitation according to the following procedure: First about 1 mol dm^{-3} of aqueous titanium tetrachloride ($TiCl_4$) solution was prepared. Then a prescribed amount of lanthanum nitrate ($La(NO_3)_3 \cdot 6H_2O$) was dissolved in a proper volume of the aqueous $TiCl_4$ solution to form a transparent mixed solution. The transparent mixed solution was then hydrolyzed to form a mixed precipitate consisting of $TiO(OH)_2$ and $La(OH)_3$ by adding 7 mol dm^{-3} aqueous ammonia solution very slowly under vigorous stirring until the pH value of the reaction system was higher than 9.33; under which the La^{3+} ions in the mixed solution are considered to be precipitated fully ($La^{3+}<10^{-5}$ mol dm^{-3}). After the pH reached the required value, the reaction system was continuously stirred for 30 min at room temperature to obtain a homogeneous precipitate in compositions, and then placed for next separation. The mixed precipitate was separated by centrifuge and rinsed three times using a 0.5 mol dm^{-3} aqueous ammonium solution to remove the NH^+_4 and Cl^- ions in the precipitate. The rinsed precipitate was then vacuum dried at 70 °C for more than 24 h and ground to powder; next the powder was calcinated in an electric furnace at a prescribed temperature for more than 2 h. After the furnace cooled down to room temperature, the sample was taken out and ground to form La^{3+}-TiO_2 photocatalysts. Each sample with the same doping amount was prepared in duplicate, and used for the tests of photocatalytic activity separately.

La^{3+}-TiO_2 photocatalysts prepared by sol–gel process

The sol–gel process was also used to prepare La^{3+}-TiO_2 catalysts for comparison. The La^{3+}-TiO_2 samples were prepared by a sol–gel process with the following procedure: solution A was prepared by dissolving an amount of tetrabutyoxytitanium (TBT) into two thirds of ethanol under stirring, according to the molar ratio of n(TBT): n(C_2H_5OH): n(H_2O) = 1:20:0.8, and solution B was prepared by mixing the residual one third of the ethanol with the prescribed amount of water in which a prescribed amount of $La(NO_3)_3 \cdot 6H_2O$ was dissolved . The pH of solution A was first adjusted to 1 ~ 2 by dropping nitric acid in and under stirring for 10 min, then the solution B was added into the solution A very slowly under vigorous stirring to form a clear yellowish sol; after that the reaction system was continuously stirred for 30 min. The sol was then stored at room temperature (25–30 °C) to form gel, and the gel was vacuum dried at 60 °C for at least 24 h to remove the water and organic solvents in the gel. Finally the dried gel was ground and calcinated in an electric furnace at different temperatures for 2 h. After the furnace cooled down to room temperature, the samples were taken out and ground to form La^{3+}-TiO_2 photocatalysts. Each sample with the same doping amount was also prepared and used for the tests of photocatalytic activity as mentioned above.

Photocatalytic activity testing

The photocatalytic activities of the La^{3+}-TiO_2 catalyst samples were tested by using Rhodamine B as a model chemical of degradation. The degradation tests were preliminarily conducted in a simple stirred slurry photoreactor to widely investigate the doping effect and preparation conditions. The testing procedure was as follows: 20 cm^3 of Rhodamine B solution with a concentration of 10 mg dm^{-3} was put into the reactor, and then 0.2 g of photocatalysts was added into the 20 cm^3 test solution under magnetic stirring. The suspension system was mixed for 15 min in the dark to disperse the photocatalysts fully and to reach adsorption equilibrium, then the mixture was illuminated for degradation. Some papers have proved that the degradation of most organic compounds and Rhodamine B using lanthanide or iron-doped TiO_2 photocatalysts could reach a steady state at ca. 1 h [19, 27, 28, 31]. So in this work, the suspension was illuminated for 1 h by a 50 W medium pressure mercury lamp from the side of the reactor, and then the suspension was centrifuged at 15,000 rpm for 5 min to obtain clear supernatant. The concentration of Rhodamine B solution was detected using a UV-2000 UV–Vis spectrometer at the largest adsorption wavelength $\lambda = 553$ nm, then the degradation efficiency of Rhodamine B can be calculated on the basis of concentration change. Photocatalytic tests for each sample were conducted in duplicate, and the averaged value was used for evaluation of photocatalytic activity.

It is known that heterogeneous photocatalytic reactions with TiO_2 catalysts are affected not only by light irradiation but also oxygen transfer (as electron acceptor). In order to get more accurate photocatalytic data and check the repeatability of photocatalytic activity of the samples, photoactivity tests were further carried out in an air lift photoreactor with 0.038 m inside diameter and 0.265 m height, the configuration of which is similar to that in the literature [33]. A draft tube with 0.018 m inside diameter and 0.15 m height was installed to obtain good dispersion of the catalyst samples; it consists of a vertical Pyrex tube with a glass filter gas-sparger for aeration. Preliminary experiments showed that when the flow rate of air was larger than 0.8 dm^3 min^{-1}, uniform dispersion of the catalysts were achieved, and the photocatalytic reactions in this reactor are not affected by oxygen transfer. The testing procedure was as follows: 200 cm^3 of Rhodamine B solution with a concentration of 10 mg dm^{-3} was put into the photoreactor, then air was injected into the reactor at 0.8 dm^3 min^{-1}, making the solution circulate between the inner tube and reactor wall, then the catalyst sample was added into the test solution at a weight/volume ratio of 2 g dm^{-3}. The suspension system was circulated for 30 min in the dark to disperse the photocatalysts fully and to establish adsorption equilibrium. Then the mixture was symmetrically illuminated by two 50 W medium pressure mercury lamps from the side of the reactor (the distance from the centerline of the lamps to the reactor wall was 0.1 m). Subsequent procedure was the same as mentioned above.

Dark adsorption

To investigate the adsorption behaviour of some typical La^{3+}-TiO_2 powder samples, a set of Rhodamine B adsorption isotherm tests were carried out in the dark with the following procedure: 10 cm^3 of Rhodamine B solutions with different initial concentrations were added with 0.1 g of La^{3+}-TiO_2 powders, and then put into a shaker operated at 150 rpm for 24 h at 25 °C. After adsorption tests, the mixtures were centrifuged at 15,000 rpm for 5 min to obtain clear supernatants, which were used for determining the equilibrium concentrations of Rhodamine B solutions. The amounts adsorbed at different conditions could be calculated on the basis of concentration changes before and after the adsorption tests. Each test at a same condition was done in duplicate.

Characterization of La^{3+}-TiO_2 catalysts

To determine the crystal phase composition of the prepared La^{3+}-TiO_2 catalysts, X-ray diffraction measurement was carried out at room temperature using a diffractometer (D/MAX-IIIC) with Cu K_α radiation ($\lambda = 0.15406$ nm). An accelerating voltage of 20 kV, emission current of 20 mA and scanning speed of 2 deg min^{-1} were used. The surface area of the La^{3+}-TiO_2 catalysts were measured by nitrogen adsorption, by the dynamic BET method, using a Beckman Coulter Sorption Analysis System (SA 3100). Before adsorption, the samples were outgassed in an evacuation chamber for 20 min at 120 °C. The BET surface area was determined by multipoint BET method using the adsorption data in the relative pressure (P/P_0) range of 0.0527–0.18. The desorption isotherm was used to determine the pore size distribution using the Barret–Joyner–Helender (BJH) method with cylindrical pore size. The pore volume can be checked out from the cumulative pore volume distribution curve; differential pore volume distribution data were used to calculate average pore size and size distribution. To know the dispersion state of catalysts in the process of photocatalytic reactions, the average particle size and particle size distribution of the catalyst powders were determined in water medium using a light-scattering particle analyzer in the range of 0.02–1200 μm (Rise-2008 made by Jinan Rise Co. China). The catalyst samples were ultrasonically dispersed in distilled water and the particulate morphology of La^{3+}-TiO$_2$ catalysts was observed by a scanning electron microscope (JEOL, JSM-6460 LV). The surface elemental analysis of the catalysts was conducted by electron probe micro analyzers (JEOL, JMS-8800).

Results and discussion

Photocatalytic activities of the La^{3+}-TiO$_2$ catalysts

A lot of preliminary experimental results of photocatalytic degradation of Rhodamine B obtained in the simple stirred slurry photoreactor indicated that La doping in TiO$_2$ seems to enhance photocatalytic activity at a lower concentration range (0–2.0 wt.%), and that the La^{3+}-TiO$_2$ catalysts prepared by coprecipitation exhibited obviously higher photocatalytic activities than those prepared by a conventional sol–gel process; the effectiveness of doping lanthanum in TiO$_2$ showed a strong dependency both on heat treatment temperature and doping amount. Furthermore prolonging calcination time (>2 h) did not cause an increase in the photocatalytic activity of the La^{3+}-TiO$_2$ catalysts (data not shown). The more accurate data of Rhodamine B degradation obtained in the air lift photoreactor is shown in Fig. 1 using the catalysts prepared by coprecipitation and sol–gel processes. The S in Fig. 1 represents the standard deviation of two experimental results for the repeatedly prepared catalysts with a same lanthanum doping amount. It could be seen that again, the experimental results further verified the obvious differences in photocatalytic activity obtained in the preliminary tests.

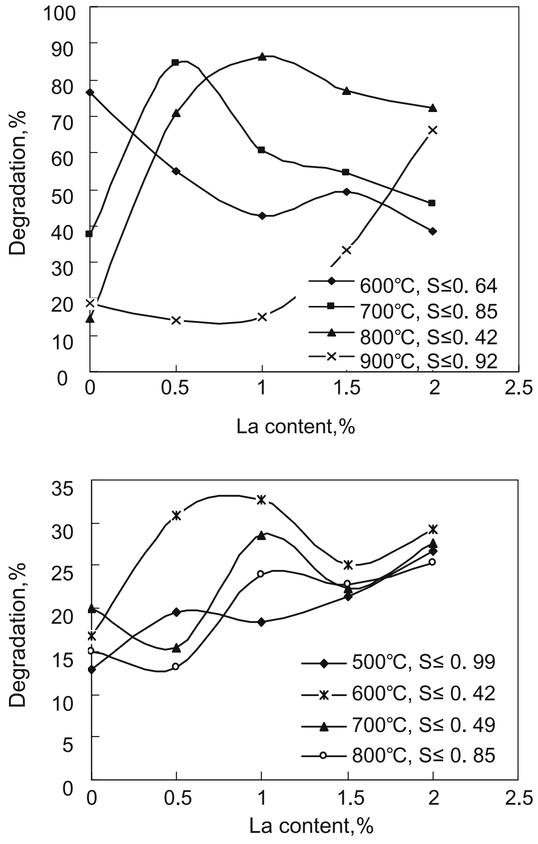

Fig. 1 The photocatalytic degradation efficiencies of Rhodamine B obtained in the air lift photoreactor using coprecipitation prepared catalysts (top) and sol–gel prepared catalysts (bottom). The calcination time for all samples is 2 h. S in the legends represents standard deviation of experimental data

It was believed that a lot of Ti–O atomic arrangement defects would act as centres for the recombination of photoinduced electron–hole pairs, and that a regular crystal structure is the prerequisite for TiO$_2$ semiconductor as an effective photocatalysts [32]. A higher calcination temperature is beneficial for the completion of the solid phase reactions and formation of regular crystal structure of the La^{3+}-TiO$_2$ catalysts, thus facilitating an increase in photocatalytic activity. Conversely, if the calcination temperature is so high as to cause the formation of a lot of rutile TiO$_2$ in the catalysts, the photocatalytic activity of the catalysts will decrease because it is known that the photoactivity of rutile is lower than that of anatase TiO$_2$; therefore, there must be an optimum calcination temperature. It seems from this work that 700–800 °C is a better calcination temperature range for coprecipitation method, and 600 °C is a better calcination temperature for sol-gel method, higher or lower temperatures than that range will lead to a decrease of photoactivity. Qian et al. [34] studied the effects of La doping on the microstructure and photoactivity of TiO$_2$ using a sol–gel process and obtained an optimum heat treatment temperature of 600 °C, which is the same as that obtained in this work. In addition, Ranjit et al. [27–28] used 550 °C of heat treatment temperature in sol–gel process and got La^{3+}-TiO$_2$ photocatalysts with good photocatalytic activity.

Xu et al. [29] reported that the amount of lanthanide doping is an important factor affecting photocatalytic activity, and the optimum amount of lanthanide doping was ca. 0.5 wt.% in sol–gel process. Li et al. [31] also prepared La^{3+}-TiO$_2$ photocatalysts by the sol–gel process, and found the optimum amount of lanthanum doping was ca. 1.2 wt.%. Therefore it appears that the optimum amount is related to preparation conditions, and that the optimum amount of lanthanum doping may be from 0.5 wt.% to 1.2 wt.% for a sol–gel process. In this work, it can be seen from Fig. 1 that the optimum doping amount is from 0.5 wt.% to 1.0 wt.% at the optimum calcination temperature 600 °C for a sol–gel method, which agrees very well with that reported by the above. Furthermore, using the coprecipitation method, a La^{3+}-TiO$_2$ photocatalyst with excellent photoactivity could be prepared at calcination temperature 700–800 °C; calcination time is 2 h and the corresponding optimum La doping amount is also 0.5–1.0 wt.% (upper one of Fig. 1), which is in accordance with that reported for the sol–gel processes. Different photocatalytic activities come from the different chemical and physical properties of the as-prepared photocatalysts; so what are the differences that need to be checked by adsorption experiments and structure characterization of some typical samples prepared at the optimum conditions?

Adsorption properties of the optimum catalysts

It could be seen from Fig. 1. that the catalysts with the optimum photocatalytic activities can be prepared by the coprecipitation process at La doping amount 1.0 wt.% under the heat treatment temperature of 800 °C (abbreviated as COP1.0%La^{3+}-TiO_2-800), and by the sol–gel process at 1.0 wt.% under 600 °C (abbreviated as SG1.0% La^{3+}-TiO_2-600). In order to investigate the differences leading to the different photocatalytic activities a set of adsorption tests were conducted in the dark. The Rhodamine B adsorption isotherms on the optimum samples are shown in Fig. 2. by plotting C/Γ versus C, which were fitted by the Langmuir adsorption model [31] as follows:

$$C/\Gamma = C/\Gamma_{\max} + 1/(K_a \cdot \Gamma_{\max}) \qquad (1)$$

where C is the equilibrium concentration of Rhodamine B in the solution in mg dm^{-3}, K_a is adsorption equilibrium constant in dm^3 mg^{-1}, and $\Gamma_{\max}$ is the saturated adsorption capacity in mg g^{-1}.

The values of $\Gamma_{\max}$ and K_a were obtained from the above fitting and are listed in Table 1. The results indicated that the adsorption of Rhodamine B on the catalysts follows the Langmuir adsorption equation very well. The coprecipitation prepared samples have lower saturated adsorption capacity, but almost the same adsorption constants in comparison with the sol–gel prepared samples. From the L-H relationship: $R = kKC/(1 + KC)$ [29], where R is the reaction rate, k is the rate constant and K is the adsorption equilibrium constant, the adsorption effects of the optimum photocatalysts prepared by the coprecipitation and the sol–gel process should have almost the same contribution to the overall reaction rate because of the similar adsorption constants. In other words, the fundamental cause leading to the obviously different degradation efficiencies of Rhodamine B lies in the reaction rate constant k, which is then determined by the internal chemical and physical properties of the catalysts.

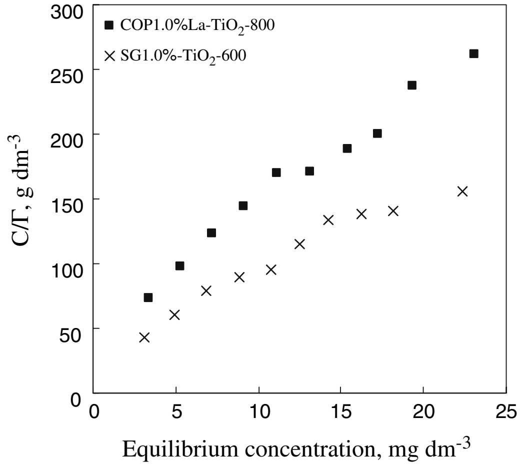

Fig. 2 The adsorption isotherms of Rhodamine B on the optimum photocatalysts

Table 1 The saturated adsorption capacity and adsorption equilibrium constant of La^{3+}-TiO_2 in Rhodamine B solutions

Photocatalysts	Saturated adsorption capacity $\Gamma_{\max}$, mg g^{-1}	Adsorption equilibrium constant Ka, dm^3 mg^{-1}	Relative coefficients, R^2
COP1.0%La-TiO_2-800	0.1091	0.1742	0.9807
SG1.0%La-TiO_2-600	0.1658	0.1774	0.956

XRD study

XRD was used to investigate the differences in crystal phase composition and the average crystallite size of the optimum La^{3+}-TiO_2 powders prepared by the coprecipitation and the sol–gel process, respectively. The XRD patterns are shown in Fig. 3, which indicated that the diffraction peaks of the COP1.0%La-TiO_2-800 are sharper than that of the SG1.0%La-TiO_2-600. This implied that the

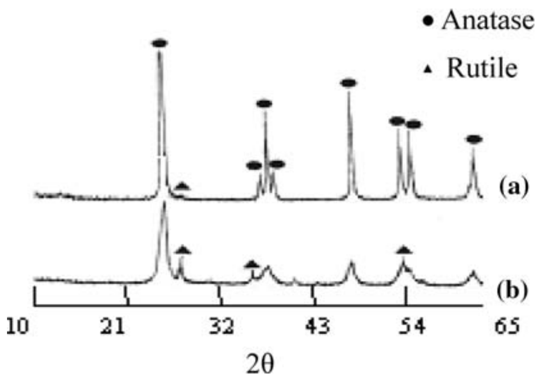

Fig. 3 XRD patterns of the optimum La^{3+}-TiO_2 photocatalysts. (**a**) COP1.0%La-TiO_2-800, crystallite size 22.96 nm. (**b**) SG1.0%La-TiO_2-600, crystallite size 17.22 nm

grain size of COP1.0%La-TiO_2-800 is bigger than that of SG1.0%La-TiO_2-600. Based on the XRD data, the crystallite sizes of the optimum samples were calculated using the Scherrer formula: $D = 0.89\lambda/\beta\cos\theta$ [29]. The grain sizes of COP1.0%La-TiO_2-800 and SG1.0%La-TiO_2-600 are 22.96 nm and 17.22 nm, respectively. The grain size of 17.22 nm for the SG1.0%La-TiO_2-600 sample is very close to that (17.66 nm) for the 1.2 wt.% La-TiO_2 samples reported by Li et al. [31]. The difference in grain size should be ascribed to the different heat treatment temperatures because higher calcination temperature will facilitate the growth and agglomeration of fine grains.

However, what is especially worthy of attention from Fig. 3 is that the crystal phase of COP1.0%La-TiO_2-800 catalysts was absolutely dominated by anatase although a calcination temperature as high as 800 °C was used in this process. In contrast, the crystal phase of the SG1.0%La-TiO_2-600 samples had considerable amount of rutile in it although the calcination temperature for the sol–gel process was 200 °C lower than that for the coprecipitation (the characteristic diffraction peaks of rutile appeared at $2\theta = 27.6$, 36.4 and 54.45°). Similarly, the grain size of the rutile could be estimated using the Scherrer formula, and is about 7.07 nm. Generally speaking, the phase change from anatase to rutile occurs in the temperature range of 600–1100 °C [28]. It was reported that the lanthanum doping of TiO_2 can inhibit the phase transformation and increase of crystal size in a sol–gel process [27, 31]. So our work has demonstrated that the inhibition effect of lanthanum doping is related to doping process, and that the inhibition effects are greater using the coprecipitation process rather than using the sol–gel process. This finding is beneficial for preparing the anatase La^{3+}-TiO_2 catalysts with more regular crystal structure through a higher heat treatment temperature, as shown in Fig. 3.

Why there was a different inhibition effect of lanthanum doping in the two processes might be related to the different precursors for the formation of La^{3+}-TiO_2 catalysts. More research has proved that lanthanide doping of TiO_2 can decrease the crystallite size [27–29, 31]. The decrease in particle size can be attributed to the presence of Ti–O–La and Sm–O–Ti bonds or lanthanide oxide particles at the interfaces in the doped samples, which prevents anatase particles from adhering together, and inhibits the growth of crystal grains [28–29, 31]. According to the report by O-venstone and Yanagisawa [35], a critical particle size is required for the anatase to rutile transformation. Thus the mechanism for the inhibition effect of lanthanum doping on the phase transformation is realized through the inhibition of grain growth. A greater inhibition effect of grain growth also leads to a greater inhibition of phase transformation. In the coprecipitation prepared precursor, there could be much more Ti–O–La bonds than in the sol–gel prepared precursor because it was composed of the hydroxides of titanium and lanthanum which are similar in chemical structure. In contrast, the sol–gel prepared precursor was composed of the partially hydrolyzed TBT and nitrate of lanthanum which is different in chemical structure. The more Ti–O–La bonds in the coprecipitation prepared precursor increased the inhibition effect of grain growth greatly, which in turn enhance the inhibition effect of phase transformation from anatase to rutile.

It was reported that the crystallinity of TiO_2 photocatalysts is a major factor affecting photocatalytic activity [32]. The sharper diffraction peaks of the COP1.0%La-TiO_2-800 samples also showed their higher crystallinity or more perfect crystal structure. Therefore, one of the reasons for the higher photocatalytic activity of the La^{3+}-TiO_2 samples prepared by the coprecipitation might be attributed to its more regular anatase structure, which was obtained through a higher calcination temperature.

On the other hand, the crystalline phase of the titania catalyst is an important factor that determines its activity [27–28]; this was also verified by our work. When the heat treatment temperature was increased from 800 °C to 900 °C for the La^{3+}-TiO_2 samples prepared by the coprecipitation, the photocatalytic activity decreased sharply (Fig. 1) due to the formation of a lot of rutile (in this case, the transformation from anatase to rutile for the 1.0 wt.% La^{3+}-TiO_2 samples began at 800 °C, as shown in Fig. 3a). So the reason for the lower photocatalytic activities of the SG1.0%La-TiO_2-600 could be the presence of the rutile phase.

BET surface areas and pore size distribution

The BET surface areas and pore size distributions of the two optimum photocatalysts, i.e. COP1.0%La-TiO_2-800 and SG1.0%La-TiO_2-600 samples were measured in this work to investigate the physical factors leading to the different photocatalytic activities. All the results are shown in Fig. 4 and listed in Table 2. It could be seen that the pore sizes of the COP1.0%La-TiO_2-800 samples are obviously larger than that of the SG1.0%La-TiO_2-600 samples, and the average pore size of the former is almost four times that of the latter. All the pores in the SG1.0%La-TiO_2-600 samples were in the range of mesopores (2–50 nm), but those in the COP1.0%La-TiO_2-800 samples basically consist of 75% mesopores and 25% macropores (>50 nm). This may be caused by the different calcination temperatures. The formation of mesoporous structure in the samples was attributed to the aggregation of TiO_2 particles [36, 37]. The smaller pores in the sample endured much greater stress than the bigger pores, so the smaller pores collapsed first during calcinations; and the aggregation of

Table 2 The BET surface area, pore volume and pore size distribution of the optimum La^{3+}-TiO_2 samples

Samples	BET surface area, $m^2\ g^{-1a}$	Pore volume, $cm^3\ g^{-1b}$	Pore size distribution^c					
			D_{av}, nm	D_{10}, nm	D_{25}, nm	D_{50}, nm	D_{75}, nm	D_{90}, nm
COP1.0%La-TiO_2-800	14.9	0.121	32.5	18.9	28.2	36.9	44.6	57.6
SG1.0%La-TiO_2-600	36.7	0.075	8.2	4.5	5.7	7.7	10.4	24.9

[a] The BET surface area was measured by multipoint BET method using the adsorption data in the relative pressure (P/P_0) range of 0.0547–0.181

[b] Pore volume and average pore size were calculated based on the data of change of differential nitrogen adsorption volume with pore size using statistic method in the range of 3.195 to 119.2 nm for the COP1.0%La-TiO_2-800 samples and 3.197–121.3 nm for the SG1.0%La-TiO_2-600 samples

[c] D_{av} denotes the average pore size of the samples

[d] D_x means the volume percentage of the pores with diameter smaller than D_x nm in total pore volume does not exceed x%, e.g. for the COP1.0%La-TiO_2-800 sample, D_{10} = 18.88 nm means the volume percentage of the pores with diameter smaller than 18.88 nm in total pore volume does not exceed 10%

bigger crystallites could form bigger pores. Therefore, increasing calcination temperature caused the pores to become bigger [38].

The BET surface area of the SG1.0%La-TiO_2-600 samples was more than two times that of the COP1.0%La-TiO_2-800 samples (36.71 vs. 14.89 $m^2\ g^{-1}$), implying that it could have a larger adsorption capacity. This was verified by the adsorption test results, as shown in Table 1 (saturated adsorption capacity is 0.1658 vs. 0.1091 mg g^{-1}). Generally speaking, the large surface area of the catalysts should be beneficial to the enhancement of photocatalytic activity, but the results of the photocatalytic degradation tests were contrary to expectation, indicating that the differences in surface area cannot be a controlling factor in influencing the photocatalytic activity. Ranjit et al. [28] compared the surface area and photocatalytic activity of Yb_2O_3/TiO_2 with that of Eu_2O_3/TiO_2 and PrO_3/TiO_2, and came to the same conclusion.

According to the adsorption test results, the two samples had similar adsorption equilibrium constants (0.1742 and 0.1774 $dm^3\ mg^{-1}$), although their surface areas differed greatly. This illustrated that the adsorption of Rhodamine B on the catalysts could be dominated by chemisorptions. Similarly, the surface complexes of Ln^{3+}-salicylic acid and Ti^{4+}-salicylic acid were checked on lanthanide doped TiO_2 photocatalysts showing that the tendency for the formation of Ln^{3+}-salicylic acid complexes is higher than that for Ti^{4+}-salicylic acid [28]. This further implied that the distribution of lanthanum ions in the two catalyst samples had a similar tendency.

On the other hand, it is worthy of attention that the COP1.0%La-TiO_2-800 samples had larger pore volume and much bigger pores in comparison with the SG1.0%La-TiO_2-600 samples. Bigger pores are beneficial to the mass transfer in the catalysts, helping to enhance the rate of photocatalytic degradation. However, most photoreactions take place on the catalyst surface, so the bigger pores present in the COP1.0%La-TiO_2-800 samples should not be the main factor leading to higher photocatalytic activity.

Particle size distribution and SEM observation

The dispersion of sample powders in the slurry reaction system is very important because it provides a direct contact area between catalyst particles and substrates. The particle size distributions of the sample powders were detected with water medium after 1 min of ultrasonic

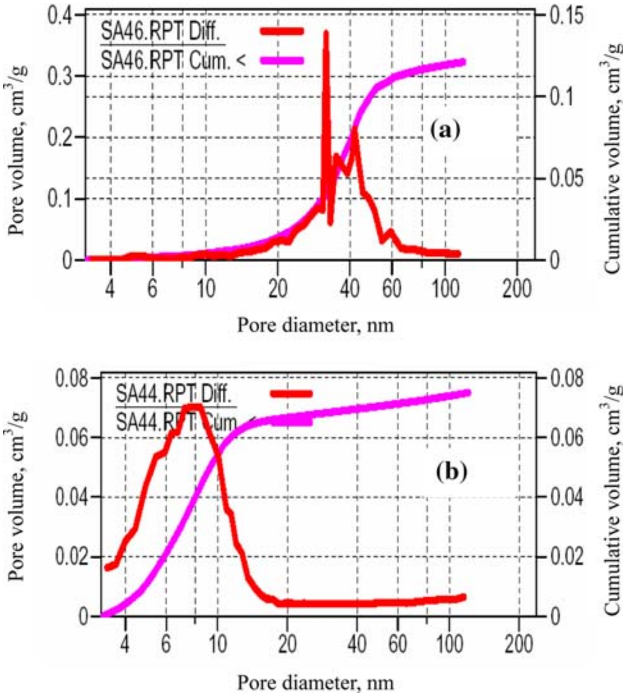

Fig. 4 Pore size distribution curves of the samples. (**a**) COP1.0%La-TiO_2-800; (**b**) SG1.0%La-TiO_2-600

dispersion. The results indicated that the two sample powders almost had the same particle size distribution in water medium, as shown in Fig. 5, illustrating very similar dispersion properties for the two catalysts. Using mathematic statistic methods, the average particle sizes can be calculated. They are 18.82 and 17.25 μm for the COP1.0%La-TiO_2-800 and SG1.0%La-TiO_2-600 samples, respectively.

SEM was also used for the direct observation of particle size and morphology of the optimum catalyst powders. As shown in Fig. 6, the two samples consisted of more fine particles and agglomerates (2–20 μm), but the particle morphology is very different. Most of the COP1.0%La-TiO_2-800 particles are spheroid or oblate spheroid and look looser-and some macropores could be observed on some particles: this agrees with the results of the BET surface and pore size tests. In contrast, the SG1.0%La-TiO_2-600 sample had some flakes and rectangular particles which look denser, indicating that there may be some mesopores in the particles. The results of the observation of the pores on the catalyst particles agree well with the results of the BET surface, pore tests mentioned above. The difference in the morphology might be caused by the different precursors of the La-TiO_2 catalysts.

Element analysis of the La^{3+}-TiO_2 photocatalysts

The surface element composition of the optimum catalyst samples was analyzed by an electronic probe microanalyzer. Two main elements, Ti and O, were found on the surface of the catalysts, and the atomic ratio of O to Ti is ca. 2.49 for the 1.0 wt.% La^{3+}-TiO_2 photocatalysts, regardless of the preparation process. Li et al. [31] reported a 2.70 of the atomic ratio of O to Ti for 1.2 wt.% La^{3+}-TiO_2 catalysts prepared by sol–gel processes. A higher O content might be attributed to the presence of La_2O_3 on the surface of the photocatalyst particles. The [O]/[Ti] ratio obtained in this work agreed very well with that reported by Li et al. because it was found that the ratio of [O]/[Ti] on the surface of the photocatalysts increased with the increase of lanthanum ion doping [31].

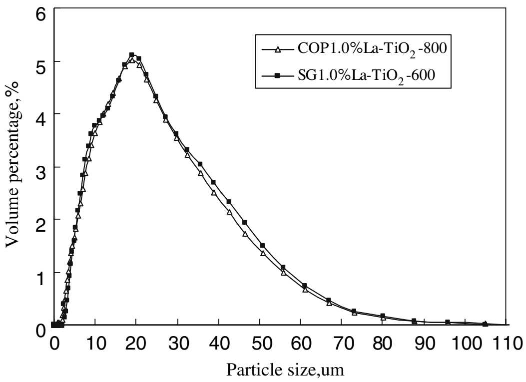

Fig. 5 Particle size distribution of the sample powders within water after 1 min of ultrasonic dispersion

The same [O]/[Ti] ratio on the surface of the two optimum photocatalysts does not mean that the surface chemical states of the La^{3+}-TiO_2 catalysts prepared by the coprecipitation and the sol–gel process are the same. Li et al. [31] found that there were four elements, Ti, O, C and La, on the surface of the La^{3+}-TiO_2 catalysts prepared by the sol–gel process. But the photocatalysts obtained in the coprecipitation should only have three elements of Ti, O and La, because there are no reactants containing carbon atoms in this process. According to the literature [31], there are Ti^{3+} ions on the surface of the La^{3+}-TiO_2 catalyst because of the diffusion of titanium into the lattice of lanthanum oxide and the reduction of Ti^{4+} by residual carbon during heat treatment. For the coprecipitation method, there was no reduction of Ti^{4+} by the residual carbon during heat treatment, so the content of Ti^{3+} on the surface of La^{3+}-TiO_2 catalysts prepared by this process could be lower than that by the sol–gel process.

The La^{3+}-TiO_2 particles are a kind of composite photocatalyst consisting of lanthanum oxide and titanium dioxide. It was reported that the formation of a heterojunction between TiO_2 and lanthanide oxides could not prevent electron-hole recombination, and that electron transfer is not possible from the conduction band edge of TiO_2 to La_2O_3 because the potential of conduction band edge of La_2O_3 (about –1.8 to –3.5 eV versus standard hydrogen electrode (SHE)) is lower than that of TiO_2 (about –0.3 eV versus SHE for anatase) [26, 31]. However, more investigations have, in fact, proved the more efficient separation of electron-hole pairs in La^{3+}-TiO_2 particles than in pure TiO_2 [26–29, 31]. According to the research by Li et al. [31], the modification of the surface state of the catalysts might be another critical reason for promoting the efficient separation of electron–hole pairs; in particular a limited amount of oxygen defects (OV) and Ti^{3+} species on surface or in bulk can suppress the recombination of electron–hole pairs. The presence of surface OV facilitates the formation of superoxide anions O_2^- upon chemisorption of oxygen, and anions O_2^- then act as hole traps. The Ti^{3+} species are first oxidized by the adsorbed oxygen into Ti^{4+} species, which then act as electron traps as follows:

$$Ti^{3+} + O_2(gas) \rightarrow \ Ti^{4+} + O^{2-}(ads) \tag{2}$$

$$Ti^{4+} + e^-_{cb} \rightarrow Ti^{3+} \tag{3}$$

$$O_2^- + 2h^+_{vb} \rightarrow 2^{\cdot}OH \tag{4}$$

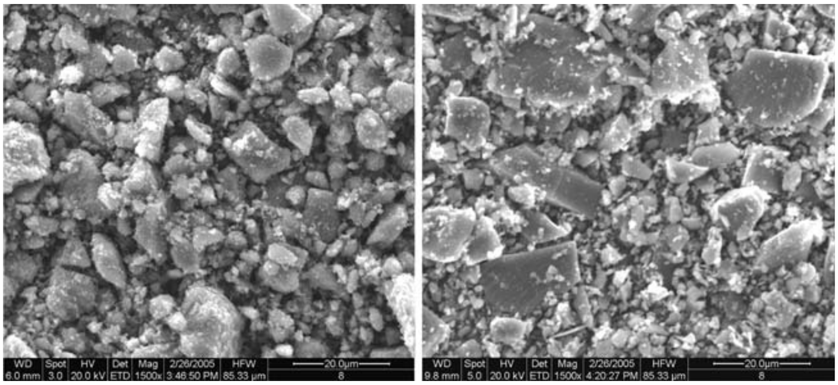

Fig. 6 The SEM micrographs of the optimum catalyst samples. Left one: COP1.0%La-TiO_2-800; Right one: SG1.0%La-TiO_2-600

In addition, charge transfer from the surface to oxygen also plays an important role in hindering the electron–hole recombination [39].

Although the Ti^{3+} ions on the surface of La^{3+}-TiO_2 catalysts play significant roles in changing photocatalytic properties and enhancing photoactivity, there must be an optimum content. Higher content of Ti^{3+} on the surface of La^{3+}-TiO_2 catalysts acts as the charge-carrier recombination centre, advances the recombination of photoinduced electron–hole pairs, and causes the decrease of photoactivity [31]. Therefore, the difference in the content of Ti^{3+} species on the surface of the La^{3+}-TiO_2 catalysts prepared by coprecipitation and sol–gel processes could be another important factor causing the different photocatalytic activity, but this needs to be further confirmed in a subsequent work.

Conclusion

The preparation of La^{3+}-TiO_2 photocatalysts by a coprecipitation process was for the first time investigated in this work. It was found that the La^{3+}-TiO_2 photocatalysts prepared by coprecipitation exhibited an excellent photocatalytic activity as compared with that prepared by the usually used sol–gel process. The optimum photocatalysts prepared by the coprecipitation and sol–gel process have similar adsorption equilibrium constants in Rhodamine B solution and particle size distribution in water medium although there are larger differences in their surface area, morphology and pores, verifying the chemisorption on the surface of the catalyst particles. The pores in the sol–gel prepared catalysts are in the range of mesopores (2–50 nm), whereas the pores in the coprecipitation prepared catalysts consist of bigger mesopores and macropores (>50 nm). The morphology of the primary particles and agglomerates of the La^{3+}-TiO_2 catalyst powders was affected by doping processes. The experiments demonstrated that the inhibition effect of lanthanum doping on the phase transformation is greater in the coprecipitation process than in the sol–gel process, which could be related to the different amount of La–O–Ti bonds in the precursors for forming La^{3+}-TiO_2 catalysts. This finding is beneficial for preparing the anatase La^{3+}-TiO_2 catalysts with more regular crystal structure through a higher heat treatment temperature. The optimum amount of lanthanum doping is ca. 1.0 wt.% for the both preparation processes. The surface atomic ratio of [O]/[Ti] is ca. 2.49 for 1.0 wt.% La^{3+}-TiO_2 catalysts prepared by the two processes. These results agreed very well with the results obtained in a typical sol–gel process [31]. The obviously higher photocatalytic activity of the La^{3+}-TiO_2 samples prepared by the coprecipitation could be mainly attributed to their more regular anatase structure and more proper surface chemical state of Ti^{3+} species. The optimum preparation conditions are 1.0 wt.% doping amount of lanthanum ions, calcination temperature 800 °C and calcination time 2 h for the coprecipitation process.

Acknowledgements This research is supported by the fundamental research projects of Chongqing Institute of Technology and Chongqing Science and Technology Commission.

References

1. Noorjahan M, Durga KV, Subrahmanyam M, Boule P (2004) Appl Catal B: Environ 3:209
2. Lee JH, Kang M, Choung SJ (2004) Water Res 3:713
3. Ohno S, Sato D, Kon M (2003) Thin Solid Films 2:207
4. Kawahara T, Ozawa T, Iwasaki M, Tada H (2003) J Colloid Interface Sci 2:377
5. Kwon CH, Kim JH, Jung IS, Shin H (2003) Ceramics Int 8:851
6. Kominami H, Kumamoto H, Kera Y (2003) J Photochem Photobiol A: Chem 1/2:99
7. Nakashima T, Ohko Y, Kubota Y, Fujishima A (2003) J Photochem Photobiol A: Chem 1/2:115
8. Villacres R, Ikeda S, Torimoto T, Ohtani B (2003) J Photochem Photobiol A: Chem 1/2:121
9. Ohno T, Tokieda K, Higashida S, Matsumura M (2003) Appl Catal A: Gen. 2:383
10. Watson S, Beydoun D, Amal R (2002) J Photochem Photobiol A: Chem 1–3:303

11. Yin S, Li RX, He QL, Sato T (2002) Mater Chem Phys 1–3:76
12. Jung KY, Park SB, Ihm SK (2002) Appl Catal A: Gen 1/2:229
13. Jin S, Shiraishi F (2004) Chem Eng J 2/3:203
14. Di P, Agatino GL, Elisa MG (2004) Appl Catal B: Environ 3:223
15. Yamashita H, Harada M, Misaka J (2003) Catal Today 3/4:191
16. Sugiyama K, Ogawa T, Saito N (2003) Surf Coat Technol 174–175:882
17. Takeuchi M, Onozaki Y, Matsumura Y (2003) Nucl Instrum Methods Phys Res Section B. 206:259
18. Rampaul A, Parkin IP, O'Neill SA, Souza JD, Mills A (2003) Polyhedron 1:35
19. Yan PF, Zhou DR, Wang JQ (2002) Chem J Chinese U 12:2317 (in Chinese)
20. Liu HY, Gao L (2004) J Am Ceramic Soc 8:1582
21. Wu SX, Ma Z, Qin YN (2004) Acta Phys Chim Sin 2:138
22. Ihara T, Miyoshi M, Iriyama Y, Matsumoto O, Sugihara S (2003) Appl Catal B: Environ 4:403
23. Dana D, Vlasta B, Milan M, Malati MA (2002) Appl Catal B: Environ 2:91
24. Di PA, Garcıa LE, Ikeda S (2002) Catal Today 1–4:87
25. Hu C, Tang YC, Tang HX (2004) Catal Today 3/4:325
26. Ranjit KT, Willner I, Bossmann SH, Braun AM (2001) Environ Sci Technol 7:1544
27. Ranjit KT, Cohen H, Willner I, Bossmann S, Braun AM (1999) J Mater Sci 34:5273
28. Ranjit KT, Willner I, Bossmann SH, Braun AM (2001) J Catal 204:305
29. Xu AW, Gao Y, Liu HQ (2002) J Catal 2:151
30. Matsuo S, Sakaguchi N, Yamada K, Matsuo T, Wakita H (2004) Appl Surf Sci 1–4:233
31. Li FB, Li XZ, Hou MF (2004) Appl Catal B: Environ 48:185
32. Xie YB, Yuan CW, Li XZ (2005) Mater Sci Eng B3:325
33. Kimura T, Yoshikawa N, Matsumura N, Kawase Y (2004) J Environ Sci Health Part A 11–12:2867
34. Qian SW, Wang ZY, Wang MQ (2003) J Mater Sci Eng 1:48 (in Chinese)
35. Overstone J, Yanagisawa K (1999) Chem Mater 11:2770
36. Yu JG, Yu JC, Leung MKP, Ho WK, Cheng B, Zhao XJ, Zhao JC (2003) J Catal 217:69
37. Huang W, Tang X, Wang Y, Koltypin Y, Gendanken A (2000) Chem Commun 1415
38. Yu JG, Zhou MH, Cheng B, Yu HG, Zhao XJ (2005) J Mol Catal A: Chem 227:75
39. Mills A, Morris S (1993) J Photochem Photobiol A: Chem 71:75